

# Confirmation of an Electron Avalanche Causing Laser-induced Bulk Damage at 1.06 $\mu\text{m}$

D. W. Fradin, Eli Yablonovitch, and Michael Bass

Measurements have been made on intrinsic optical bulk breakdown in ten alkali halides at 1.06  $\mu\text{m}$  and in one at 0.69  $\mu\text{m}$ . By comparing the results to previously reported experiments conducted at 10.6  $\mu\text{m}$  and at direct current, it has been possible to identify the damage mechanism as electron avalanche breakdown. Self-focusing has been controlled by restricting the probe powers to well below the critical powers for catastrophic self-focusing, and damage from inclusions has been distinguished from intrinsic damage. Implications of this work for surface damage studies are explored.

## I. Introduction

When the intensity of light propagating in an initially transparent medium is sufficiently high, the medium will be disrupted. This phenomenon, called laser-induced breakdown,<sup>1</sup> may be described by the following sequence of steps: First, absorption occurs at microscopic absorbing inclusions<sup>2</sup> or by means of an intrinsic nonlinear absorption process such as multiphoton absorption or electron avalanche breakdown. Second, the energy absorbed from the beam heats the medium. Finally, a thermally induced fracture or a phase change occurs that in solids results in permanent material damage.

Experimental studies of intrinsic laser breakdown processes can be seriously misinterpreted if catastrophic self-focusing occurs in the medium<sup>3</sup> or if absorbing inclusions are present in the irradiated volume. Since self-focusing results in a greatly enhanced beam intensity, experiments in which it occurs cannot accurately measure the level of irradiation for intrinsic laser breakdown. The apparent bulk damage thresholds deduced from such experiments are a measure of threshold for self-focusing and not for laser breakdown. The presence of absorbing inclusions having diameters  $>0.1 \mu$  in the irradiated volume can dominate the damage process.<sup>2,4</sup> Such inclusions are probably the most common cause of laser damage especially when large volumes are irradiated. Experimental data must therefore be recorded in a manner that permits ac-

curate identification of inclusion breakdown as distinguished from intrinsic breakdown in order to study the latter unambiguously.

Recent work at 10.6  $\mu\text{m}$  indicates that intrinsic damage can be isolated.<sup>5</sup> For laser beam power well below the critical power for self-focusing, catastrophic beam collapse cannot occur and corrections due to the index nonlinearity are quite small.<sup>6,7</sup> The high intensities necessary for laser breakdown can be achieved at low powers by strong external focusing, which, as an additional advantage, often allows the probe beam to avoid inclusions. Microscopic inspection of the damaged volume can then be used to distinguish inclusion from intrinsic breakdown.

The alkali halide family is a natural choice for laser-breakdown studies. Besides being useful infrared optical materials, these compounds are transparent from about 15  $\mu\text{m}$  to about 0.2  $\mu\text{m}$ , so that linear absorption does not present a problem. In addition, because they have been studied extensively to determine their response to applied fields at dc<sup>8</sup> and at 10.6  $\mu\text{m}$ ,<sup>5</sup> comparative studies can be made.

In this paper we present measurements of intrinsic bulk laser breakdown in ten different alkali halide crystals at 1.06  $\mu\text{m}$ , which were obtained under experimental conditions that preclude both self-focusing and absorbing inclusions as the causes of damage. The data show striking similarities among 1.06  $\mu\text{m}$ , 10.6  $\mu\text{m}$ , and dc breakdown measurements, indicating that an avalanche breakdown process,<sup>9</sup> essentially in its dc limit, is responsible for intrinsic damage at 1.06  $\mu\text{m}$ .

Since self-focusing may reach threshold before breakdown at optical frequencies,<sup>3</sup> it is important to understand both the conditions under which catastrophic self-focusing occurs and the corrections from the index nonlinearity when a catastrophic focus is prevented. For this reason an analysis of self-focusing is outlined in the appendices, and the general re-

---

The first two authors named were with the Gordon McKay Laboratory, Harvard University, Cambridge, Massachusetts 02138 when this work was done; E. Yablonovitch is now with Bell Telephone Laboratories, Murray Hill, New Jersey 07974. M. Bass is with Raytheon Research Division, Waltham, Massachusetts 02154.

Received 22 September 1972.

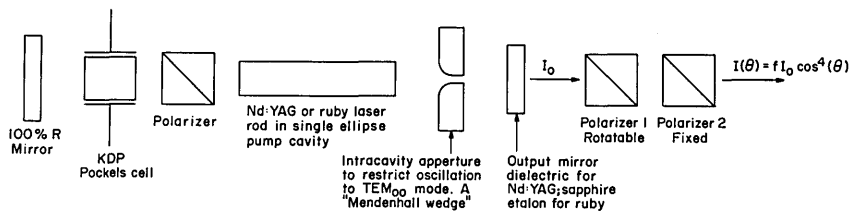


Fig. 1. Laser and variable attenuator configuration for damage studies.

sults relevant to our measurements are discussed in Sec. II.A. Confirming theoretical predictions that catastrophic self-focusing is absent, two important experimental checks are then reported. We present in Sec. II.B the results of a series of carefully controlled experiments in which intrinsic bulk damage in alkali halides was measured. A well-characterized TEM<sub>00</sub> mode laser beam with total power more than one order of magnitude below calculated critical powers for self-focusing was tightly focused within the samples in order to obtain the high intensities needed for damage. Then, in Sec. II.C we show how the experimental results can be fully explained in terms of avalanche breakdown.

## II. Experiments

### A. Lasers and Beam-Handling Optics

Figure 1 shows schematically the principal features of the laser damage source. The experiments were performed using a pulse-pumped, electrooptically Q-switched, Nd:YAG laser. Some important properties of this device are summarized in Table I. Figure 2 shows that the Nd:YAG laser output was in the lowest-order Gaussian or TEM<sub>00</sub> mode.

The time structure of the pulses from the laser appears reasonably smooth when reviewed with a fast photodiode oscilloscope combination having a measured risetime of 0.5 nsec. We have conducted Fabry-Perot studies and have found that normally fewer than four adjacent modes are oscillating simultaneously, so that the time structure is effectively fully resolved. Longitudinal mode selection is accomplished by aligning the faces of the plane-parallel laser rod parallel to the 100% R resonator mirror. Despite the low reflectivity of the antireflection-coated rod surfaces, the high gain of the rod and the high reflectivity of the mirror create an effective intracavity reflector.

To verify that the transverse mode structure on axis is constant with time, the center of the beam was sampled with a 25- $\mu$  pinhole and found to have the same time structure as the entire beam. The stability on axis was found to be superior to that of the spatially integrated power.

The breakdown data were taken by focusing through a 13-mm focal length lens to approximately 2 mm inside the samples. Care was taken to ensure that spherical aberrations from both the lens and the plane entrance surface of the sample being tested were unimportant. A fast photodiode was used to

monitor the transmitted light, and an energy monitor recorded the energy in each laser pulse.

The combination of one rotatable and one fixed polarizer resulted in a variable light attenuator that was highly sensitive, quite reproducible, and that did not affect the laser pulse's polarization, spatial distribution, or duration. If the fixed polarizer is oriented to transmit the laser polarization and if  $\theta = 0^\circ$  is the angle of the rotating polarizer that gives maximum transmission through this attenuator, the transmitted intensity at any other angle of rotation about the beam axis is  $I(\theta) = bI_0 \cos^4\theta$ , where  $I_0$  is the incident light intensity and  $b$  is the fraction transmitted when  $\theta = 0^\circ$ . Calibrated neutral-density filters were often used in conjunction with the variable Glan attenuator.

### B. Self-Focusing

A laser beam propagating in a transparent medium induces an increase in the index of refraction by an amount proportional to the laser intensity. At powers in excess of some critical power this nonlinearity causes the intensity distribution to become unstable, and a catastrophic beam collapse results.

Self-focusing may occur as the result of a number of nonlinearities. In solids, for Q-switched laser pulses, the process that normally leads to the smallest value of critical power and hence dominates self-focusing is electrostriction.<sup>6</sup> This is the case for the alkali halides where thermal and electronic contributions to self-focusing are much smaller than the electrostrictive effect and can be neglected.<sup>10,11</sup>

An intense light wave whose power lies below a critical power  $P_c$  will not experience a catastrophic collapse in a nonlinear medium because although focusing by self-action will always be present, diffrac-

Table I. Laser Parameters

	Nd:YAG 1.06 $\mu$ m	Ruby 0.694 $\mu$ m
Energy TEM <sub>00</sub> Mode	1.5 mj	2.0 mj
Beam Diameter at Output Mirror TEM <sub>00</sub> Mode	0.8 mm	0.7 mm
Polarization	Linear	Linear
Pulse Repetition Rate	1 pps	1 pulse/5 sec
Pulse Duration in TEM <sub>00</sub> Mode	4.7 nsec (FWHP)	14 nsec (FWHP)
Pulse to Pulse Energy Reproducibility	$\pm 7\%$	$\pm 10\%$

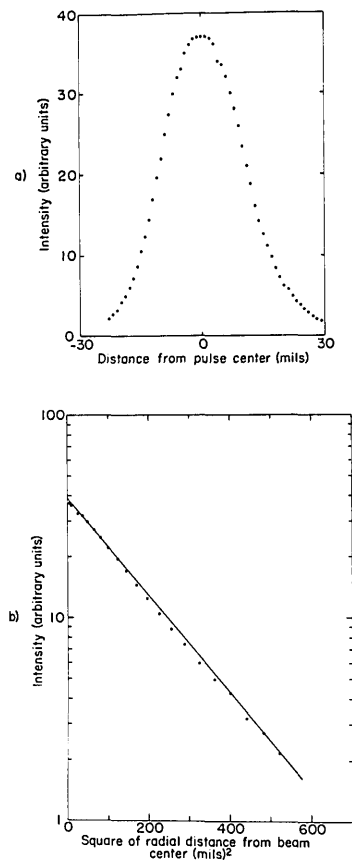


Fig. 2. Intensity distribution of the YAG laser as a function of radial distance from the beam center at the position of the focusing lens.

tion acts in the opposite sense to cause divergence and dominates at such powers.<sup>7</sup> At powers sufficiently far below  $P_c$ , therefore, the intensity distortion due to the index nonlinearity can be treated as a constant perturbation on diffraction effects and usually neglected. These observations allow us to effectively eliminate self-focusing by restricting probe powers to well below calculated critical powers while focusing strongly by external optics to reach the field intensities necessary to cause optical damage.

Theoretical self-focusing parameters are defined and derived in the appendices, where quantitative corrections from the index nonlinearity at powers below  $P_c$  are discussed. Table II summarizes the numerical results. The probe power is the experimental peak power on axis and is more than one order of magnitude below  $P_c$ . From a purely theoretical viewpoint, therefore, catastrophic self-focusing is impossible, and it can be shown that beam distortion from the index nonlinearity introduces at most a few percent correction in the measured electric field strengths. If catastrophic self-focusing does occur, the breakdown damage data are a measure of the critical powers rather than intrinsic breakdown field. The measured threshold intensity will then scale with the square of the calculated focal diameter if the process is steady state and will depend on the

pulse width if the process is transient. (The diameter dependence in the steady state results from the existence of a constant critical power  $P_c$  that does not vary with beam diameter.)

To test our belief that self-focusing was absent we conducted two experiments. In the first the relative field strength threshold for damage in NaCl was measured with three different focusing lenses, corrected for spherical aberrations, and having focal lengths of 1.3 cm, 2.5 cm, and 3.8 cm. The experiment was conducted at 1.06  $\mu\text{m}$ . If steady-state self-focusing were present, the observed damage threshold would have scaled with the inverse of the focal length. It did not, and, in fact, to within 5% the field strength was independent of focal length. This effectively eliminated the possibility of steady-state self-focusing. Since  $t_p/\tau \geq 1$  from Table II, self-focusing should not be transient. Eq. (A15), however, predicts the results observed when transient self-focusing is present. For this reason a measurement was made of the damage threshold as a function of pulse duration with the beam diameter held essentially constant.

By changing the pumping level for the YAG laser, we were able to extend the pulse width by a factor of 2.3–10.8 nsec. In addition, the breakdown strength at 0.69  $\mu\text{m}$  was measured with ruby laser pulses of 14-nsec duration and a focused diameter 25% smaller than that obtained with the YAG laser. The same 1.3-cm focal length lens was used in all three measurements, and to compute the ruby value, we assumed the same transverse intensity variation as that present at 1.06  $\mu\text{m}$ . To within 15% no change was noted in the threshold field despite the pulse-width dependence in Eq. (A15). The agreement for the ruby pulses was especially reassuring, because the critical power varies with wavelength squared. If transient self-focusing were present, we would have seen a change by a factor of 18 in the measured intensity—an effect that would have been quite dramatic. A factor of 9 comes from the pulse-width dependence of the transient critical power and a factor of 2 from the wavelength dependence.

Table II. Calculated Steady-State, Self-Focusing Parameters and Experimental Values of Pulse-Widths and Peak Power

	Wavelength (microns)	$\tau$ ( $10^{-9}$ sec)	$t_p$ ( $10^{-9}$ sec)	$n_2 \times 10^{22}$ (mks)	$P_{cr}$ ( $10^3$ watts)	$P_c$ ( $10^3$ watts)	$P_{input}$ ( $10^3$ watts)
	10.6	5.5	200		48,000	175,000	120
NaCl	1.06	2.7	4.7	2.3	480	1,750	50
	0.69	2.0	14		204	746	26
	10.6	11.2	200		13,200	50,000	20
RbI	1.06	5.4	4.7	8.1	132	500	8.1
	0.69	4.0	14		56	203	—

For  $P_{input} < P_c$  catastrophic self-focusing will not occur.

The 10.6  $\mu\text{m}$  data is taken from reference 6.

See appendices for definitions of  $\tau$ ,  $n_2$ , and  $P_{cr}$ . To convert  $n_2$  to esu units, multiply by  $0.91 \times 10^9$ .

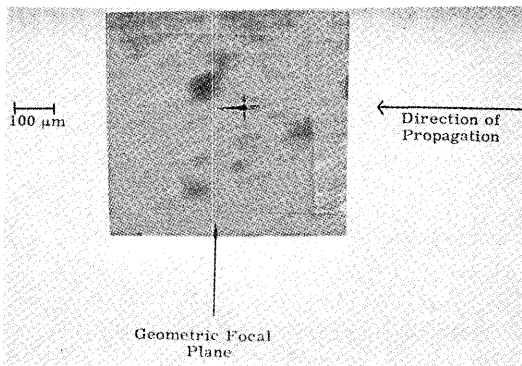


Fig. 3. Intrinsic Damage in RbCl.

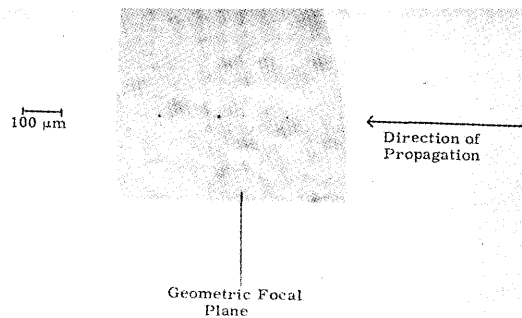


Fig. 4. Inclusion damage in RbCl.

Perhaps the best experimental check for self-focusing is the actual measurement of breakdown strengths. Self-focusing theory appears to be totally unable to account for the experimental results given below in which both relative and absolute values of breakdown strengths show striking similarities to  $10.6\text{-}\mu\text{m}$  values. We thus conclude that prior to the onset of material damage, self-focusing has been effectively eliminated as a competing nonlinearity.

The possibility may exist that self-focusing occurs after a sufficient number of electrons have been generated to cause intense local heating of the sample. We note, however, that in our measurements any late developing nonlinearity is unimportant.

### C. Experimental Measurements of Breakdown

#### 1. Damage Measurements at $1.06\ \mu\text{m}$

To measure the breakdown strengths of the alkali halides, we focused the laser beam approximately 2 mm into each sample and recorded the number of laser pulses necessary to produce internal damage at various power levels. In every case where damage occurred, a white spark was produced, and the damage was later carefully inspected with a microscope. Because of the small volume damaged by our highly focused  $1.06\text{-}\mu\text{m}$  pulses (less than  $2 \times 10^{-5}\ \text{mm}^3$ ), a large number of data points could be taken with each sample (40 to 100).

Defining threshold as that value of incident power necessary to produce intrinsic damage in a single shot for 50% of the positions probed,<sup>5</sup> we calculated the rms, on-axis electric field at the measured threshold in NaCl. Corrections were made for reflections from various surfaces and the changes in the beam diameter due to the effect of the index nonlinearity. This was the basic calibration, and all other values of threshold were measured relative to  $E_{\text{NaCl}}$ . In order to avoid errors from daily power fluctuations and possible alignment changes, a single sample of NaCl was tested with each alkali halide. It was readily determined that a slight misalignment of the focusing lens (13-mm focal length) had no measurable effect on the relative breakdown strengths.

Visual inspection and the breakdown statistics suggested that spatial inhomogeneities from inclusions were not affecting the results except in the single case of RbCl. Damage that we regarded as intrinsic consisted at each damage position of a single pointed region that began at the geometrical focus and extended a very short distance back toward the laser, increasing in cross section to give a teardrop appearance. A typical example is indicated in Fig. 3. In RbCl, on the other hand, regions with low breakdown thresholds consisted typically of one or more spherical voids randomly distributed about the focus (Fig. 4). A number of points, however, did appear visually to have intrinsic damage and were consistently more difficult to break down. These data points were used for the RbCl results.

Finally, a fast-photodiode detector system with a 0.5-nsec risetime monitored the transmitted light as shown in Fig. 5 and was used to confirm threshold levels in NaCl and KCl as well as to establish the approximate time structure and stability of the laser output.

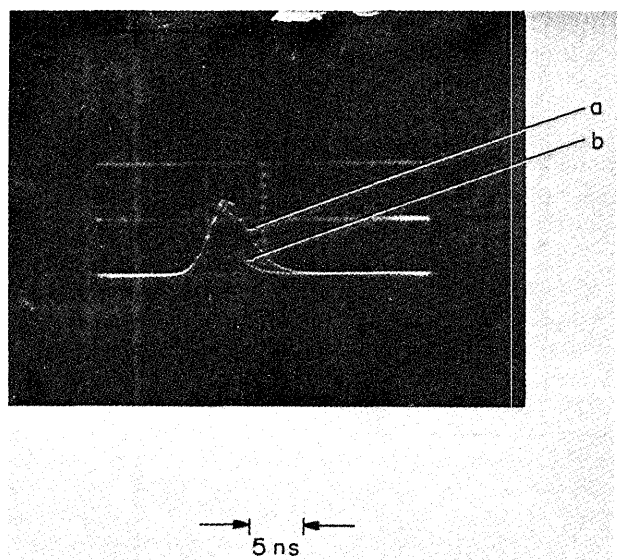


Fig. 5. Nd:YAG laser pulse transmitted through the sample.

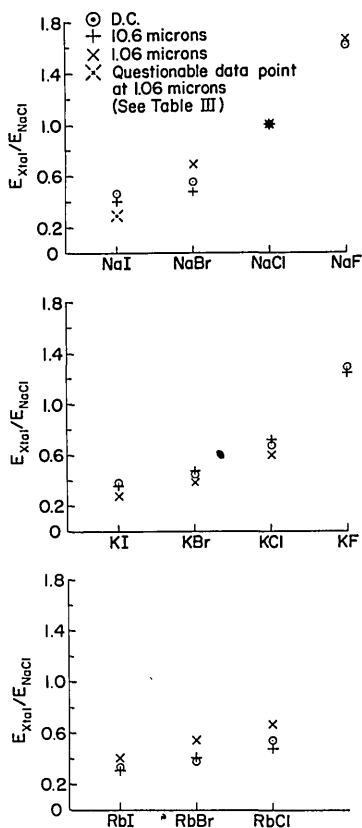


Fig. 6. Comparison of breakdown strengths for various alkali halides studies at dc, 10.6  $\mu\text{m}$  and 1.06  $\mu\text{m}$

Values for the breakdown field obtained at 1.06  $\mu\text{m}$  are summarized in Fig. 6 and in Table III along with both the 10.6- $\mu\text{m}$  data collected by Yablono-vitch<sup>5</sup> and accepted dc results.<sup>8</sup> These results are normalized to the respective values of field necessary to damage NaCl listed in Table IV. This allows the striking similarity in trends of breakdown field to be easily observed and the possible systematic deviations at 1.06  $\mu\text{m}$  to be recognized. The quoted errors at 10.6  $\mu\text{m}$  are  $\pm 10\%$ , and our random experimental errors in relative fields are estimated to be no more than  $\pm 10\%$  with possible errors due to microscopic strains adding another  $\pm 5\%$ . Two different samples of both NaCl and KBr from two different manufacturers gave nearly identical results.

Careful statistics for variations in the breakdown strength were collected on NaCl because of the high quality of the two samples that we obtained. It was found that within experimental error the damage process in NaCl is thresholdlike. Though larger fluctuations were noticed for other materials, the uncertainties are considered to result from surface imperfections, internal strains, and laser fluctuations. No measurement of any probabilistic nature of breakdown was made.

Some evidence for intrinsic fluctuations, however, was found by monitoring the light transmitted through the samples. On several occasions a laser pulse produced damage in the same position where a

more intense pulse one second before had been focused without damaging the sample. While these observations may have resulted from unresolved time structure in the second laser pulses, the same observations were made at ruby wavelength where Fabry-Perot studies indicated that the pulses were normally free of such fluctuations.

## 2. Damage Measurement at 0.69 $\mu\text{m}$

The breakdown strength of NaCl was also measured with a ruby laser to confirm the absence of self-focusing as noted in Sec. II.B. Table IV records the average of about fifty damage measurements. Although the laser was normally operating in a single longitudinal mode as indicated by Fabry-Perot and photodiode studies, each laser shot during the measurement was monitored with a fast photodiode and recorded.

In Fig. 7 time-resolved photographs of transmitted light indicate the sudden attenuation normally seen for laser pulses that caused damage. Because of the smooth time structure of most of the pulses, we were able to record a few cases in which the instant of first attenuation, considered to be the onset of material damage, occurred after the peak of the laser pulse had passed. An example is given in Fig. 7(c). The same effect was observed at 1.06  $\mu\text{m}$ . This may be explained both by invoking a statistical model for breakdown<sup>9</sup> or by the considerations of a time-dependent avalanche discussed in the next section.

Table III. Relative Breakdown Fields—Normalized to  $E_{\text{NaCl}} \approx 2 \times 10^6 \text{ V/cm}$

	NaI	NaBr	NaCl	NaF
DC	0.460	0.553	1	1.60
10.6 $\mu\text{m}$	0.405	0.476	1	
1.06 $\mu\text{m}$	(0.29) <sup>a</sup>	0.67	1	1.64
	KI	KBr	KCl	KF
DC	0.380	0.460	0.667	1.27
10.6 $\mu\text{m}$	0.369	0.482	0.713	1.23
1.06 $\mu\text{m}$	0.27	0.38	0.57	
	RbI	RbBr	RbCl	
DC	0.327	0.387	0.553	
10.6 $\mu\text{m}$	0.323	0.400	0.472	
1.06 $\mu\text{m}$	0.40	0.55	0.67	

<sup>a</sup>Crystal was extremely hygroscopic and no final check was made with the microscope to determine if inclusions were responsible for the damage observed.

Table IV. Absolute Breakdown Strength of NaCl

$E_{\text{peak}}(\text{dc})$	$1.50 \times 10^6 \text{ V/cm}$	
$E_{\text{rms}}(10.6 \text{ microns})$	$1.95 \times 10^6 \text{ V/cm}$	$\pm 10 \text{ Percent}$
$E_{\text{rms}}(1.06 \text{ microns})$	$2.3 \times 10^6 \text{ V/cm}$	$\pm 20 \text{ Percent}$
$E_{\text{rms}}(1.06 \text{ microns})^a$	$2.2 \times 10^6 \text{ V/cm}$	$\pm 20 \text{ Percent}$

<sup>a</sup>Gaussian profile assumed.

An rms field of  $2 \times 10^6 \text{ V/cm}$  inside NaCl at 1  $\mu\text{m}$  corresponds to a peak incident intensity of about  $16 \times 10^7 \text{ watts/cm}^2$ .

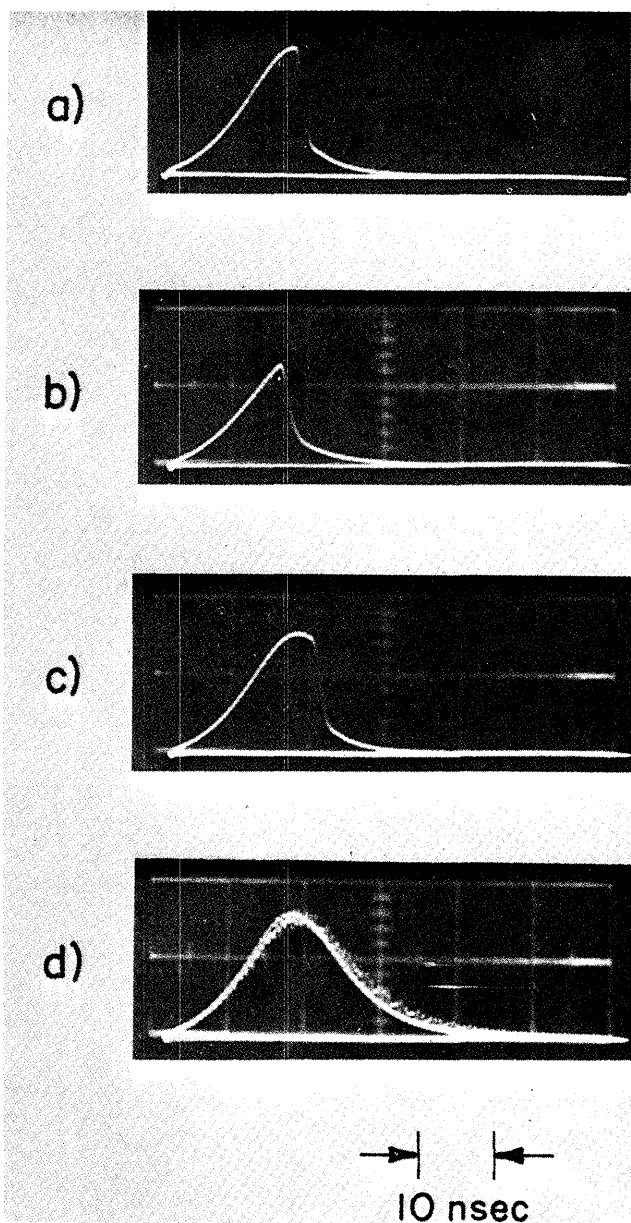


Fig. 7. Ruby laser pulses transmitted through NaCl sample. A  $TEM_{00}$  mode ruby laser with total pulse energy of 0.3 mJ was focused inside the inclusion-free sample with a 14-mm focal length lens. (a) Damaged when peak laser field was reached,  $E_{\text{Damage}}/E_{\text{Peak}} = 1$ . (b) Damaged before peak laser field was reached,  $E_{\text{Damage}}/E_{\text{Peak}} = 0.896$ . (c) Damaged after peak laser field was reached,  $E_{\text{Damage}}/E_{\text{Peak}} = 0.954$ . (d) Three successive pulses, no damage,  $E_{\text{Peak}} \equiv 1$  (arbitrary units).

### III. Discussion

#### A. Bulk Damage

The experiments reported here were performed under carefully controlled conditions using stable, well-characterized lasers and optical systems for which aberrations were unimportant. Because we were able to probe each sample in many different positions, random fluctuations in breakdown strength were averaged out. It was possible to distinguish

between inclusion and intrinsic damage by inspection of the residual damage and to correct for the effects of inclusions in the one material for which they were important. In addition, experimental tests showed that catastrophic self-focusing was absent and, consistent with theory, that the index nonlinearity did not affect the results to within experimental error. It is therefore concluded that the results of the 1.06- $\mu\text{m}$  and 0.69- $\mu\text{m}$  study as summarized in Fig. 6 and Table IV represent accurate measurements of intrinsic bulk damage.

Because the techniques of this study are virtually identical to those of Ref. 5, direct comparison can be made to breakdown strengths at 10.6  $\mu\text{m}$ . It has already been observed that the damage thresholds for the alkali halides at 1.06  $\mu\text{m}$  follow a trend nearly identical to that observed with the  $\text{CO}_2$  laser and, in fact, to the dc measurements of Ref. 8. It thus appears that the intrinsic process of laser-induced damage for the alkali halides has the same fundamental character as both ac damage in the infrared and dc avalanche breakdown. Moreover, the consistency of the optical breakdown strengths at 0.69  $\mu\text{m}$  suggests that this same process may dominate up to frequencies approaching  $4 \times 10^{14}$  Hz.

Data from Fig. 6 and Table IV have established the relationship  $(E_{1.06})_{\text{rms}}$  is about  $1.5 \times E_{\text{dc}}$  for ten different compounds. The precise value of the factor 1.5 is not important, since dc measurements are known to be somewhat sensitive to experimental techniques.<sup>12,13</sup> It is important, on the other hand, that consistent measuring techniques have measured the same factor of 1.5 for all ten alkali halides.

Additional support for an avalanche mechanism comes from three experimental observations concerning the time structure of the laser probe pulses. The first is that increasing the pulse width of the YAG laser output by a factor of 2.3 resulted in a 14% average drop in threshold intensity for NaCl. Averages were taken from about twenty shots at each pulse width. This change, though small, is probably real, because the test was made on a single sample of high quality NaCl and thereby avoided a major source of experimental uncertainties arising from material variations. The second observation, noted at both 1.06  $\mu\text{m}$  and 0.69  $\mu\text{m}$ , is that high frequency time structure on the pulse has little measurable effect on the breakdown strength. And finally, after adjusting the power level so that damage occurred regularly near the top of the laser pulses, the probe intensities were increased by a factor of about 3 by changing the beam attenuation. When this was done, the intensity at which the transmitted light dropped (see Fig. 7) was higher by 25% or more than it had been with the lower intensity pulses. This was interpreted to mean that increasing the effective risetime of the optical field raises the measured breakdown strength. To understand both this set of observations and the results from Table IV, some discussion of existing electron avalanche theories<sup>1,12</sup> is given.

An electron avalanche in solids is a rapid multiplication of conduction-band electrons in which an initially low density  $N_0$  of free carriers interacts with an intense electric field in the presence of phonons. The number of electrons increases with time as

$$N(t) = N_0 \exp \left[ \int_0^t \alpha(E) dt \right]. \quad (1)$$

The gain coefficient  $\alpha(E)$  is a strongly varying function whose value can be inferred from dc measurements of breakdown strength as a function of sample thickness for extremely thin specimens. For Eq. (1) to be valid the rate at which electrons are lost by trapping and diffusion out of the focal volume must be small compared to the rate at which they are generated. For  $Q$ -switched laser pulses, the electron losses are, in fact, negligible.<sup>14</sup>

Two important conclusions develop from such an analysis. The first is that the entire process of avalanche and damage involves energy exchange between the field and the electrons which is approximately described by the well-known formula for ac conductivity<sup>15</sup>

$$dW/(dt) = (Ne^2\tau)/[m(1 + \omega^2\tau^2)]E^2 \quad (2)$$

where  $N$  is the time-dependent electron density,  $\omega$  the angular frequency, and  $\tau$  the characteristic relaxation-time determined principally from phonon collisions. While this precise form of the conductivity may not be correct for polar materials such as the alkali halides, we will use it to qualitatively describe breakdown for high frequencies.

Eq. (2) shows that the energy input to the electrons scales with frequency and field as  $E^2/(1 + \omega^2\tau^2)$ , and because the details of energy input determine the electron distribution function and hence  $N(t)$ , the threshold for damage will scale in the same manner. This justifies the use of root-mean-square fields in Table IV. It also indicates that the ac breakdown strength will increase for frequencies near  $1/\tau$ . Calculation of  $\tau$  for NaCl<sup>14</sup> indicates that frequency dispersion should begin to occur somewhere near that of the ruby laser.

In dc experiments it has been observed that when the time available for the buildup of the avalanche is reduced below about 10 nsec, larger fields are needed to induce damage.<sup>14,16</sup> This may explain some of the differences between dc and laser measurements summarized in Table IV.

The field dependence of  $\alpha(E)$  in NaCl<sup>14</sup> can explain qualitatively our three time-related observations—the pulse-width dependence to breakdown, the insensitivity of threshold to fast time structure, and the increase in breakdown strength for rapidly rising pulses.

Finally, it is quite striking that the threshold field for laser breakdown is virtually identical to that for dc breakdown even though the damaged regions appear very different. To understand these two obser-

vations, it is convenient to consider the laser breakdown phenomenon in solids in two steps, energy deposition and material disruption. In our experiments the first step is by electron avalanche wherein energy is deposited at a rate given by Eq. (2). In the second step this energy deposition, which may be partially offset by thermal diffusion losses, causes the lattice temperature to rise and finally a phase change or thermally induced fracture occurs. Without the phase change or fractures there is by definition no breakdown, since no irreversible damage develops and, of course, no spark appears. This second step is geometry-dependent and determines the morphology of the damage.

In principle the threshold for damage is dependent on both steps. When inclusions cause damage, for example, the details of the thermal diffusion process that enter the problem in the second step determine the pulse-width dependence of the damage threshold.<sup>2,4</sup> On the other hand, if avalanche breakdown is the mechanism of the first step, the processes of the second step have negligible effect on the threshold field. This is a result of the highly nonlinear dependence of  $N(t)$  on the electric field. If the focusing conditions or the electrode design of one experiment make breakdown less likely by altering the processes leading to material disruption and thereby requiring a higher rate of energy deposition, this higher rate of energy input can be achieved by an immeasurably small change in the electric field strength. The apparent threshold for avalanche breakdown, therefore, will depend only on the parameters described qualitatively by Eqs. (1) and (2) and will have no measurable connection with the morphology of the damage.

## B. Implications for Surface Damage Studies

Surface damage is often a practical problem in the operation of high power lasers. For this reason a number of investigations of surface breakdown<sup>17</sup> have been made with the aim of elucidating the conditions and mechanisms of surface damage. The techniques of the studies reported here may provide a valuable tool for understanding surface damage by allowing direct comparison to bulk damage thresholds. This comparison can be made by focusing a low power laser beam first on a surface and then about 2 mm into the bulk. Because focusing problems are much less severe in the bulk and damage from inclusions can apparently be distinguished by visual observation, a stable and repeatable reference exists for surface studies. Careful investigation should help elucidate, in particular, the mechanisms responsible for surface damage under various conditions of surface preparation.

## IV. Conclusions

Careful measurements of laser-induced bulk damage have been made in ten alkali halides without the confusing effects of self-focusing. Comparison of the

results to studies at dc and at 10.6  $\mu\text{m}$  indicated that the process of ac avalanche breakdown, similar in fundamental character to dc avalanche breakdown, is responsible for the damage observed. Analysis of time-related observations confirms this conclusion.

The skillful assistance and advice of D. Bua and S. Maurici are gratefully acknowledged. We are also indebted to N. Bloembergen for valuable discussions of breakdown theory and to P. Miles for stimulating discussions of laser damage.

A report of this work under the title "Comparison of Laser-Induced Bulk Damage in Alkali-Halides at 10.6, 1.06, and 0.69 Microns" was presented at the 1972 ASTM-NBS Symposium on Laser Damage in Boulder, Colorado.

The work of D. W. Fradin and E. Yablonoitch was supported by the Joint Services Electronics Program at Harvard University under Contract N00014-67-A-0298-0006.

The work of M. Bass was supported by the Advanced Research Projects Agency of the Department of Defense and was monitored by the Air Force Cambridge Research Laboratories under Contract F19628-70-0223.

## Appendix A

To demonstrate the claim that the relative balance between diffraction and self-focusing effects is set at the entrance plane for a general steady-state nonlinearity, we calculate the curvature of the ray path from a modified, eikonal equation formalism that incorporates both diffraction effects and the steady-state nonlinearity.<sup>18</sup> Its applicability is restricted to beams with diameters  $2a$  much greater than a wavelength—a condition fulfilled in our experiments.

Writing the electric field vector  $\mathbf{E}(\mathbf{r})$  as  $\mathbf{A}(\mathbf{r}) \exp i[k\phi(r) - \omega t]$  where  $k_0 = \omega/c$  and the index nonlinearity is  $n_2 A^2$ , and ignoring terms of order  $(n_2 A^2/n_0)^2$  we can write Maxwell's equations in the simplified form

$$[(n_0 + n_2 A^2)^2 - (\text{grad}\phi)^2] \mathbf{A} + (1/k_0^2) \nabla^2 \mathbf{A} = 0. \quad *$$

If the scalar product of this equation is taken with  $\mathbf{A}$ , a term containing the factor  $1/k_0^4$  dropped, and a cross term with  $n_2 A^2$  neglected, this leads directly to an effective eikonal equation

$$n_1^2 - (\text{grad}\phi)^2 = 0, \quad (\text{A1})$$

where

$$n_1 = n_0 + n_2 A^2 + (1/2k_0^2 n_0) (\nabla^2 A/A). \quad (\text{A2})$$

In the limits of zero nonlinearity and infinitesimal wavelength, this is just the basic equation of geometrical optics. Results derived from the usual eikonal equation<sup>19</sup> can now be used with the index of refraction replaced by Eq. (A2). In particular, the curvature  $d^2\mathbf{r}/d\rho^2$  for a pencil of rays with position vector

$\mathbf{r}$  and with  $\rho$  the coordinate along the ray path is given by

$$d^2\mathbf{r}/d\rho^2 = (1/n_1)[\text{grad } n_1 - (dn_1/d\rho)(d\mathbf{r}/d\rho)]. \quad (\text{A3})$$

Equation (A3) can be simplified by restricting the treatment to cylindrically symmetric beams and by assuming that the maximum ray slope is small compared to unity. (In our experiments the maximum slope inside the sample and before the focus is less than 0.05.) Both the second term on the right in Eq. (A3) and the longitudinal component of the Laplacian in Eq. (A2) are negligible. The curvature is now expressed in a form first derived by Talanov.<sup>20</sup>

$$d^2\mathbf{r}/d\rho^2 \approx d^2\mathbf{r}/dz^2 = (1/n_1) \text{grad}_\perp n_1. \quad (\text{A4})$$

This result is important to the study of self-focusing effects because the sign of  $d^2\mathbf{r}/dz^2$  indicates whether or not the beam is converging and its magnitude is a quantitative measure of that convergence or divergence. A positive curvature results in an increase in the slope of the ray path with respect to the propagation direction and thus represents a divergence from the axis. Diffraction alone will produce a positive curvature in an isotropic medium. A negative curvature, on the other hand, will cause convergence of the beam towards the axis and indicates the dominance of the self-focusing nonlinearity.

$A^2(r)$  is proportional to the light intensity, and where the beam propagates with little or no change in shape, the intensity is equal to the power in the beam divided by the beam area  $\pi a^2(z)$ . Let  $p$  be an effective power that absorbs these proportionality constants, including the factor  $\pi$  in the beam area. (This effective power has, in fact, a functional form—it may be Gaussian ( $\exp[-2r^2/a^2]$ ), for example—and it is this functional form that describes the beam shape.) We can therefore consider  $p$  to be a function of a radial variable that is independent of the beam size. Defining the coordinate  $x$  as  $x = r/a(z)$ , we can write

$$A^2(r) = p(x)/a^2(z) = \text{effective power/beam area}. \quad (\text{A5})$$

Equation (A5) is normally assumed in numerical calculations and has been referred to as the *constant shape approximation*.<sup>21</sup> Along with Eq. (A4) it provides the basic relationships to calculate the critical power, the self-focusing length, and the quantitative influence of the index nonlinearity when diffraction dominates.

By expanding  $\nabla^2_\perp$  in cylindrical coordinates  $r$  and  $z$  it is easily seen that  $\nabla^2_\perp A/A$  is also proportional to  $a^2$ . We can then write Eq. (A2) as

$$n_1 = n_0 + [1/a^2(z)]f(x), \quad (\text{A6})$$

where  $f(x)$  is the sum of contributions from both diffraction and the index nonlinearity. Since  $\text{grad}_\perp$  is

just  $a(z)^{-1}(\partial/\partial x)$ , and since  $n_1$  in the denominator of Eq. (A4) can be replaced by  $n_0$ , the derivative of  $f(x)$ , which contains no dependence on  $z$ , determines the relative importance of diffraction and self-focusing. Once this relative importance is determined for one value of  $z$ , such as  $z = 0$  at the entrance plane, it is determined for all  $z$ .

For completeness we write Eq. (A4) in the final form

$$d^2r/dz^2 = (1/n_0)[1/a^3(z)](d/dx)[f(x)], \quad (\text{A7})$$

where, using Eq. (A5),

$$f(x) = n_2(aA)^2 + [1/(2k_0^2n_0)aA][d^2(aA)/dx^2] + (1/x)[d(aA)/dx]. \quad (\text{A8})$$

The importance of neglected terms can be determined for a particular beam shape and has been shown to be negligible<sup>18</sup> except near a catastrophic self-focus or under experimental conditions where extreme external focusing is used.

The critical power  $P_c$  is in principle calculated from the requirement that the derivative  $f(x)$  vanish for all  $x$ , leading to a detailed balance of self-focusing and diffraction. Since  $f(x)$  contains no dependence on beam diameter, the critical power will not be dependent on beam diameter for a steady-state nonlinearity.

## Appendix B

The index nonlinearity leads to intensity distortions even below the critical power for catastrophic self-focusing. Using the results of Appendix A quantitative corrections from the nonlinearity can be derived.

In Eq. (A7)  $r$  is replaced by  $xa(z)$  and a new function  $g(x)$  defined. This gives

$$d^2a/dz^2 = [1/a^3(z)]g(x), \quad (\text{A9})$$

where

$$g(x) = (1/n_0x)(d/dx)f(x). \quad (\text{A10})$$

If Eq. (A9) is multiplied by  $z(da/dz)$  and integrated, we find

$$(da/dz)^2 = -[g(x)/a^2] + c, \quad (\text{A11})$$

Considerable simplification results from expanding  $A^2$  and therefore  $g(x)$  about small  $x$  and retaining terms to order  $x^2$ . In Ref. 7 this expansion is carried out for a Gaussian beam. We can investigate the geometrical focus at low powers by setting the derivative in Eq. (A11) equal to zero.<sup>7</sup> After some manipulation the focal diameter  $d$  is evaluated in terms of  $d_0$ , the diameter in absence of a nonlinearity. In particular,

$$d = d_0(1 - P/P_{cr})^{1/2}, \quad (\text{A12})$$

where  $P$  is the full power in the beam and  $P_{cr}$  is given in cgs units by

$$P_{cr} = c\lambda^2/32\pi n^2. \quad (\text{A13})$$

The result (A12) is useful for  $P/P_{cr}$  less than about 0.9. The calculated on-axis intensity at breakdown must be multiplied by a factor  $(d_0/d)^2$  to approximately correct for the effects of the nonlinearity.

More extensive analysis shows that  $P_{cr}$  is the critical power for self-focusing near the center of a Gaussian beam.<sup>21</sup> For input powers greater than  $P_{cr}$  but less than  $P_c$ , diffraction dominates everywhere except near the beam center. A collimated beam will initially intensify at such powers until the diffraction of the wings causes the on-axis intensity to drop.  $P_{cr}$  differs from  $P_c$  because the latter is a quantity averaged over the entire beam while  $P_{cr}$  is determined by the behavior near the center. In fact,  $P_c$  is not a precisely defined quantity because it is not possible to exactly balance diffraction and self-focusing over the entire beam cross section. At an input power of  $P_c$ , therefore, a propagating beam will not change its size measurably and so not experience a catastrophic self-focus, but its intensity distribution will be distorted.  $P_c$  has the same functional form as  $P_{cr}$  and differs by just a numerical factor as  $P_{cr} = 0.273 P_c$  for Gaussian beams.<sup>21</sup>

## Appendix C

The analysis of Appendix A and the results derived from it is correct only in the steady state. In solids the dominant nonlinearity is normally electrostriction, and if the process is transient, it is no longer true that the relative balance between diffraction and self-focusing is independent of propagation distance and that the critical powers are independent of beam diameter. The changes occur because electrostriction becomes nonlocal in both a temporal and a spatial sense. Although a susceptibility approach such as we have used is no longer strictly correct, it is nonetheless useful for establishing functional dependences for self-focusing parameters and approximate quantitative values.

For our experiments two results from a transient analysis are important.<sup>22</sup> The first is that transient effects decrease the effective nonlinear index  $n_2$  and thus make self-focusing more difficult. If we wish to avoid self-focusing by restricting our powers to well below the critical power, the steady-state analysis gives us a lower bound on  $P_c$ . Being in a transient regime can therefore only increase our margin of safety and improve the accuracy of our experiment by making the corrections indicated by Eq. (A12) less important.

The second important result involves the dependence of the critical power on laser pulse width and on beam diameters. In the steady state, nonlinear index  $n_2$  is given by<sup>6</sup>

$$n_2 = n_0[\rho(\partial n_0/\partial \rho)]^2/4\pi\rho v^2,$$

where  $n_0$  is the index of refraction in the absence of

the nonlinearity,  $\rho$  is the material density, and  $v$  is the acoustical sound velocity. The quantity  $[\rho(\partial n_0/\partial \rho)]$  for cubic materials such as the alkali halides may be found approximately by differentiating the Clausius-Mosotti equation. The remaining constants are tabulated in handbooks.

When the laser pulse width  $t_p$  is shorter than the electrostrictive response time  $\tau = a/v$ ,  $n_2$  is decreased in value, thereby increasing the critical power. For a triangular pulse, Kerr<sup>22</sup> has shown that

$$(n_2)_{\text{transient}} = (n_2)_{\text{steady state}}[1 - (a/v\rho)D(v\rho/a)], \quad (\text{A14})$$

where  $D(v\rho/a)$  is Dawson's integral with

$$D(\xi) = \exp(-\xi) \int_0^\xi \exp \eta^2 d\eta.$$

When  $t_p \leq \tau/2$ ,

$$(n_2)_{\text{transient}} \approx k(n_2)_{\text{steady state}}(v^2 t_p^2 / a^2).$$

This result is valid for more general and realistic pulse shapes with the numerical constant  $k$  being of order unity and having a value dependent on the precise time structure of the pulse. When this result is inserted into Eq. (A13), the critical power becomes

$$P_{c_{t_p \leq \tau}} = (P_c)_{\text{steady state}}(a^2/kv^2 t_p^2). \quad (\text{A15})$$

For short laser pulses, therefore, when the process is transient, there exists more properly a critical intensity rather than a critical power, and fairly small changes in pulse width will have a significant effect on the critical power.

As already noted, the index nonlinearity intensifies the peak on-axis intensity even at powers below the catastrophic self-focusing threshold. Using Eq. (A12), we have corrected for this effect in the calculated field strengths listed in Table IV. In addition, because of Eq. (A15) and the results of Appendix A, we can predict the diameter and pulse-width dependence to breakdown when catastrophic self-focusing is present. This information was used to evaluate the results of the self-focusing tests described in Sec. II.B.

## References

1. G. M. Zverev, T. N. Mikhailova, V. A. Pashkov, and N. M. Solovna, *Zh. Eksp. Teor. Fiz.* **53**, 1849 (1967) [*Sov. Phys.—JETP* **26**, 1053 (1968)].
2. R. W. Hopper and D. R. Uhlman, *J. Appl. Phys.* **41**, 4023 (1970).
3. C. R. Giuliano and J. H. Marburger, *Phys. Rev. Lett.* **27**, 905 (1971).
4. Yu. K. Danileiko, A. A. Manenkov, A. M. Prokhorov, and V. Ya. Khaimov-Mal'kov, *Zh. Eksp. Teor. Fiz.* **58**, 31 (1970) [*Sov. Phys.—JETP* **31**, 18 (1970)].
5. E. Yablonovitch, *Appl. Phys. Lett.* **19**, 495 (1971).
6. S. A. Akhmanov *et al.*, *Usp. Fiz. Nauk* **93**, 19 (1967) [*Sov. Phys.—Usp.* **10**, 609 (1968)].
7. G. M. Zverev and V. A. Pashkov, *Zh. Eksp. Teor. Fiz.* **57**, 1128 (1969) [*Sov. Phys.—JETP* **30**, 616 (1970)].
8. A. Von Hippel, *J. Appl. Phys.* **8**, 815 (1937).
9. M. Bass and H. H. Barrett, *IEEE J. Quantum Electron.* **QE-8**, 338 (1972).
10. N. Bloembergen, Harvard University; private communication.
11. C. C. Wang and E. L. Baardsen, *Phys. Rev.* **185**, 1079 (1969); *Phys. Rev.* **B1**, 2827 (1970).
12. For a review, see J. J. O'Dwyer, *The Theory of the Dielectric Breakdown of Solids* (Oxford U. P., London, 1964).
13. J. H. Calderwood, R. Cooper, and A. A. Wallace, *Proc. IEEE* **100**, Pt. IIA, No. 3, 1051 (1953).
14. E. Yablonovitch, Thesis, Harvard University (1972); also E. Yablonovitch and N. Bloembergen, *Phys. Rev. Lett.* **29**, 907 (1972).
15. C. Kittel, *Introduction to Solid State Physics* (John Wiley and Sons, New York, 1966).
16. D. W. Watson, W. Heyes, K. C. Kao, and J. H. Calderwood, *IEEE Trans. Elec. Insul.* **E1-1**, 30 (1965). Also, G. A. Vorobev, N. I. Lebedeva, and G. S. Naderova, *Fiz. Tverd. Tela* **13**, 890 (1971) [*Sov. Phys.—Solid State* **13**, 736 (1971)].
17. C. R. Giuliano, in *NBS Special Publication 372*, A. J. Glass and A. H. Guenther eds. (Govt. Printing Office, Washington, D.C., 1972), p. 55.
18. Chen-Show Wang, *Phys. Rev.* **173**, 908 (1968).
19. M. Born and E. Wolf, *Principles of Optics* (Pergamon Press, New York, 1959).
20. V. I. Talanov, *Zh. Eksp. Teor. Fiz. Pis. Red.* **2**, 218 (1965) [*Sov. Phys.—JETP Lett.* **2**, 138 (1965)].
21. E. L. Dawes and J. H. Marburger, *Phys. Rev.* **179**, 862 (1969).
22. E. K. Kerr, *IEEE J. Quantum Electron.* **QE-6**, 616 (1970).